Water transport in the proton-exchange-membrane fuel cell: measurements of the effective drag coefficient

G.J.M. Janssen[*], M.L.J. Overvelde

Clean Fossil Fuels, Netherlands Energy Research Foundation ECN, Post Box 1, 1755 ZG Petten, The Netherlands

Abstract

The water transport in proton-exchange-membrane fuel cells has been experimentally investigated by measurements of the effective or net drag coefficient. Results are presented for a wide range of operating conditions (current density, temperature, pressure, stoichiometry and humidity of the inlet gases), as well as for different types of membrane-electrode-assemblies. It was found that the humidity and the stoichiometry of the inlet gases had a large effect on the drag. Of the material properties investigated, the membrane thickness was found to be the most significant parameter. Inspection of the cell performances showed that drying of the cathode was much more detrimental for the cell performance than drying of the anode. This was ascribed to increased activation losses, which turned out to be extremely sensitive to the type of cathode used. © 2001 Elsevier Science B.V. All rights reserved.

Keywords: Proton-exchange-membrane fuel cell; Water transport; Dehydration; Net electro-osmotic drag coefficient

1. Introduction

The proton-exchange-membrane fuel cell (PEMFC) is considered to be an attractive power source for automotive applications as well as stationary co-generation units. With a PEMFC, high power densities can be obtained at relatively low temperatures. In addition to a high efficiency, environmental benefits are the reduction of noise and the absence of polluting emissions. However, cost and weight of the total system have to be reduced in order to make large-scale application possible. Cost effectiveness can be obtained by using alternative materials, i.e. less noble metal catalysts, cheaper materials for the electrodes, cheaper and thinner membranes, and also by reducing the need for peripheral equipment, such as a gas humidification section and compressors. The latter aspects will also reduce the weight of the system.

Of course, the advantages of cheaper materials and simpler systems must not outweigh the disadvantages of any reduction of the power density. One of the factors that are crucial for a high power density, is the water transport in the membrane-electrode-assembly (MEA). The power density can be adversely affected by too little water, i.e. drying-out, as well as by too much, i.e. flooding. The water transport in a PEMFC has been the subject of several studies, most of

which were concerned with modelling the water transport in the membrane [1–5]. Experimentally not many data are available. Staiti et al. [6] showed a distinct relation between the water transport and the amount of hydrophobic agent in the electrodes. A paper by Buechi and Srinivasan [7] deals with the water transport in cells operated on dry gases. Recently, measurements of the effective drag coefficient were reported by Choi et al. [8], but their results seem to have been obtained in a non-stationary state.

The aim of the present work was to identify the main factors that determine the water transport in a PEMFC. Therefore, the effective or net drag coefficient in PEMFCs was measured for a wide range of conditions, involving gas humidification, temperature, pressure, current density and stoichiometry. In addition, the components of the MEA were varied. The results can be used for the selection of materials and operating conditions, but they will also be used as a basis for modelling, which will be the subject of a subsequent paper [9].

2. The water transport in a PEMFC

In a PEMFC hydrogen and oxygen react electrochemically to water, producing electricity and heat. A PEMFC consists of a MEA placed between two so-called flow plates in which gas channels have been machined. The MEA

* Corresponding author. Tel.: +31-224-564803; fax: +31-224-563489.
E-mail address: janssen@ecn.nl (G.J.M. Janssen).

Nomenclature

A	active area (cm^2)
F	Faraday constant (96,485 C/mol)
j	current density (A/cm^2)
n	molar flow (mol/s)
N	molar flux (mol/s cm^2)
p	total pressure (bar)
p_{sat}	saturation pressure (bar)
$r_{d,ov}$	effective or net drag
T_{cell}	cell temperature (°C)
T_{hum}	humidification temperature of the gases (°C)
x_I	fraction of gas species I in the dry flow
λ	stoichiometry

Subscripts

w_an	water at the anode
w_back	water transported back from cathode to anode
w_cat	water the cathode
w_el,os	water transported by electro-osmosis
w_mem	water in membrane
w_prod	water produced

consists of two electrodes separated by a proton conducting membrane, usually a Nafion membrane. A schematic drawing is given in Fig. 1. At the anode side hydrogen is fed to the cell, which is electrochemically oxidised at the membrane/anode interface.

$$H_2 \rightarrow 2H^+ + 2e$$

The protons are transported through the membrane and at the membrane/cathode interface oxygen present in the air feed is reduced.

$$\tfrac{1}{2}O_2 + 2e + 2H^+ \rightarrow H_2O$$

The proton conductivity of Nafion, and therefore, the performance of the fuel cell, decreases rapidly when the water content of the membrane decreases [10]. Since the membrane easily looses water to non-saturated gases, it is essential that sufficient water is present in the gases as well as in the membrane. Water in the PEMFC can originate from three sources.

1. Humidification of the fuel inlet gas.
2. Humidification of the oxidant (air) inlet gas.
3. The electrochemical reaction in the cell.

The amount of water that is fed to the cell by humidification of the inlet anode, respectively, cathode gas is equal to

$$n_{w\_an/w\_cat}^{in} = \frac{p_{sat}(T_{hum})}{p - p_{sat}(T_{hum})} n_{H_2/air}^{in} \tag{1}$$

with

$$n_{H_2}^{in} = \lambda_{H_2} \frac{jA}{2F} \quad \text{and} \quad n_{air}^{in} = \frac{\lambda_{air}}{x_{O_2}} \frac{jA}{4F} \tag{2}$$

This means that the amount is proportional to the current density and the stoichiometry, increases with the humidification temperature and decreases with the gas pressure.

As a result of the electrochemical reactions in the cell an amount of water per time unit is produced proportional to the current density.

$$n_{w\_prod} = \frac{jA}{2F} \tag{3}$$

In a stationary state, the amount of water fed and produced per time unit is equal to the amount leaving the cell.

$$n_{w\_an}^{out} + n_{w\_cat}^{out} = n_{w\_an}^{in} + n_{w\_cat}^{in} + n_{w\_prod} \tag{4}$$
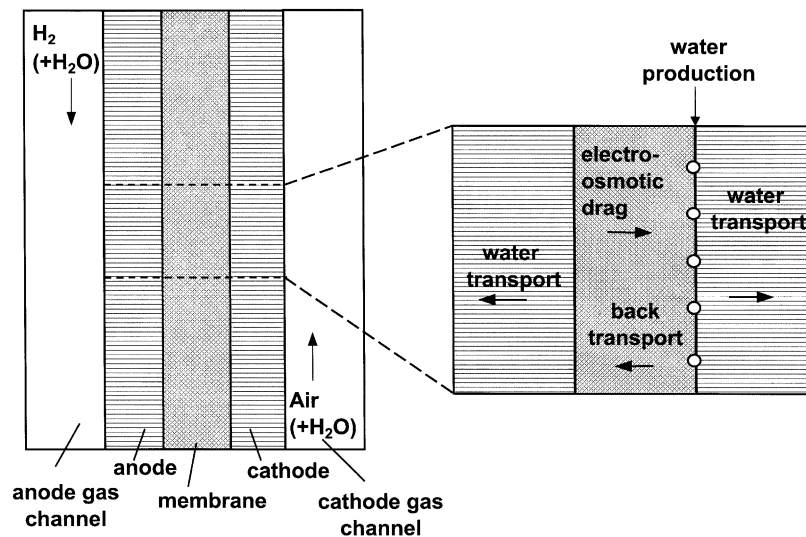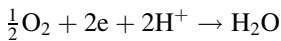

Fig. 1. Schematic representation of the water transport in a PEMFC. The direction of the water transport in anode or cathode may be reversed, depending upon the conditions.

In a PEMFC water is transported along the gas channels, but also in the direction perpendicular to the gas channels, i.e. through the membrane and the electrodes. In Fig. 1 the water transport in the PEMFC is schematically represented. When a current is drawn from the cell, protons migrate from the anode to the cathode and carry with them water molecules. The average number of water molecules transported per proton is called the electro-osmotic drag coefficient. In Nafion membranes, the value of this coefficient is between 1 (gas vapour equilibrated membranes) and 2.5 (liquid water equilibrated membranes) [11–13]. The electro-osmotic drag, together with the electrochemical production of water, results in an accumulation of water at the cathode/membrane interface. In a stationary state, the water is removed through either the cathode to the cathode gas channel or through the membrane and anode to the anode gas channel. The flux towards the anode compensates, at least in part, the electro-osmotic drag and is called the back transport. In the direction perpendicular to the membrane the following relations hold (all signs positive in the direction anode to cathode).

$$N_{w\_an} = N_{w\_mem} \tag{5}$$

$$N_{w\_mem} + N_{w\_el,os} + N_{w\_back} \tag{6}$$

$$N_{w\_mem} + N_{w\_prod} = N_{w\_cat} \tag{7}$$

The ratio of the fluxes N_{w_cat} and N_{w_an} is determined by the driving forces for both ways of water transport, i.e. the gradients in the chemical potential of water, and by the permeability of the materials. The gradients in the chemical potential of water are determined by the thickness of the components, by the water content of the membrane and the humidity of the gases. The latter in turn is dependent on the gas inlet humidification and on the temperature and pressure in the gas channel.

The back transport of water through the membrane results in a net drag of water through the membrane that is smaller than the electro-osmotic drag and can even be negative. The net drag coefficient in a cell is defined by

$$r_{d,ov} = \frac{n_{w\_an}^{in} - n_{w\_an}^{out}}{jA/F} \tag{8}$$

This means the net amount of water transported from the anode to the cathode per proton. This overall net drag can be measured by condensing and collecting the water from the anode outlet and will be used in the following to characterise the water transport in the cell.

In order to avoid dehydration, PEM cells and stacks are often operated with saturated inlet gases. This means that the cell contains excess water: product water is formed and the gases become supersaturated when gas is consumed in the chemical reaction. The amount of water contained by an exactly saturated anode outlet gas is

$$n_{w\_an}^{out} = (\lambda_{H_2} - 1) \frac{jA}{2F} \frac{p_{sat}(T_{cell})}{p - p_{sat}(T_{cell})} \tag{9}$$

and

$$n_{w\_cat}^{out} = \left(\frac{\lambda_{air}}{x_{O_2}} - 1\right) \frac{jA}{4F} \frac{p_{sat}(T_{cell})}{p - p_{sat}(T_{cell})} \tag{10}$$

In practice this means that, when gases saturated at cell temperature ($T_{hum} = T_{cell}$) enter the cell, a limited positive drag does not necessarily result in dehydration of the anode gas, whereas a substantial negative overall drag is possible before the cathode gas shows dehydration. The maximum drag before anode dehydration occurs is at these conditions given by

$$r_{max} = \frac{1}{2} \frac{p_{sat}(T_{cell})}{p - p_{sat}(T_{cell})} \tag{11}$$

and the minimum drag before cathode hydration occurs

$$r_{min} = -\frac{1}{4} \frac{p_{sat}(T_{cell})}{p - p_{sat}(T_{cell})} - \frac{1}{2} \tag{12}$$

Work by Buechi [7] among others has shown that under certain conditions operation with dry gases is possible. The criterion given in [7] for operation with dry gases is that the amount of product water should be sufficient to saturate the outlet gases, i.e.

$$\frac{1}{2} \geq \left(\lambda_{H_2} - 1 + \frac{\lambda_{air}}{2x_{O_2}} - \frac{1}{2}\right) \frac{1}{2} \frac{p_{sat}(T_{cell})}{p - p_{sat}(T_{cell})} \tag{13}$$

Fig. 2 gives the 'critical' gas stoichiometry for cell temperatures 80 and 60°C, and pressure 1.5 and 3 bar. However, satisfaction of the above equation does not guarantee that local dehydration will not occur.

3. Experimental

MEAs of 50 cm^2 were used for these experiments. A relatively large active area is needed to obtain significant amounts of water at the gas channel exits. The MEAs were
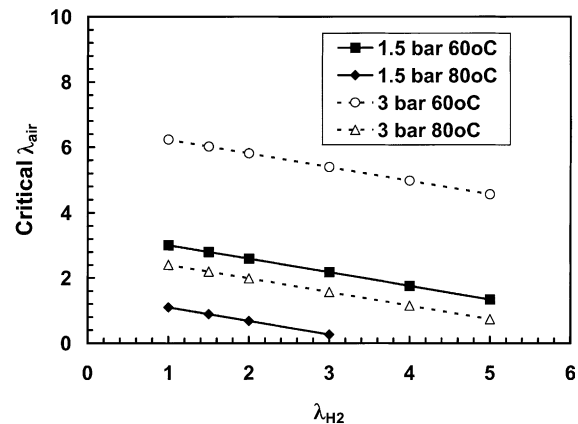

Fig. 2. The maximum air stoichiometry that for a given hydrogen stoichiometry still fulfils Eq. (13), i.e. each point corresponds to a combination of stoichiometries for which the amount of product water is just sufficient to saturate the outlet gas.

mounted between two graphite flow plates in each of which three serpentine channels had been machined with an approximate length of 0.9 m and a diameter of 1 mm. The MEA was put between two gaskets to prevent gas leaking out of the electrodes. The gaskets were chosen such that they provided optimal gas tightness.

For the gases, a counter-flow configuration was used. The pressures in the gas channels were controlled by a back-pressure regulator. The feed stream (hydrogen at the anode, air at the cathode) was either dry or humidified. In the latter case the gases were led through a water bath at cell temperature. The cells were operated for several hours (>6 h) in a constant current mode by applying an electronic load. The constant current mode enables an exact calculation of the water production (Eq. (3)) and the amount of water fed to the cell (Eq. (1)). At the exit of the gas channels the water was condensed in a cold trap and weighed. Although for calculation of the over-all drag, only the amount of water collected at the anode is necessary (see Eq. (8)), the amount of water leaving the cathode was also used to check the water balance from Eq. (4).

A list of all types of MEAs investigated is given in Table 1. In selecting the components of the MEA, a preference was given to commercially available components that are commonly used in our laboratory. This means that the results are of good practical use, but it can make comparisons of different materials less straightforward.

The membranes Nafion®105 or Nafion 112 from Dupont were cleaned in two steps: (1) for 1 h in 3% H_2O_2 at 100°C and (2) for 1 h in 1 M H_2SO_4 at 80°C. Before and after each step they were washed in an ultrasonic bath with purified water for 10 min.

Three types of electrodes were used.

1. The standard commercial E-TEK electrodes, with 0.35 mg Pt/cm^2. These will be referred to as the double-sided (E-TEK DS) electrodes, since they consisted of a carbon cloth with a thin hydrophobic microporous layer applied on both sides.
2. An electrode from E-TEK similar to the one above but with only a single thin hydrophobic microporous layer, i.e. the one supporting the catalyst (0.35 mg Pt/cm^2). This will be called the E-TEK single-sided (SS) electrode.
3. An electrode consisting of a sheet of wet-proofed TGP-H-090 (260 μm) from Toray. On the Toray paper, an ink

containing 40% Pt on Vulcan from E-TEK and Nafion solution was applied, resulting in a Pt loading of 0.5 mg/cm^2.

The catalyst layers of the electrodes were impregnated with a 5% Nafion 1100 solution from Dupont, to an amount of 1 mg/cm^2. The electrodes were hot-pressed on the membrane at 135°C for 90 s with a pressure of 40 bar.

4. Results and discussion

Below the results of the water transport measurements are presented and discussed. Most of the data were obtained at a cell temperature of 60°C. First of all the water transport in the so-called base case will be treated, i.e. a MEA consisting of two E-TEK DS electrodes and a Nafion 105 membrane (Table 1). This water transport will then be correlated to the cell performance. Next the effects of an alternative membrane and of alternative electrodes are considered. Finally, base case results obtained at a cell temperature of 80°C are presented to discuss the effect of the operating temperature. In all cases the amount of water collected at the cathode exit and anode exit was compared to the theoretical amount given by Eq. (4). Typical deviations were in the order of 4–7%.

4.1. Base cell water transport

Fig. 3 shows the net drag measured with the base case MEA. In all cases an air stoichiometry of 2 was used. The humidification of the inlet gases, the current density, the hydrogen stoichiometry and the pressure in the gas channels were varied. Fig. 3 shows a distinct relation between the humidification of the inlet gases and the measured drag.
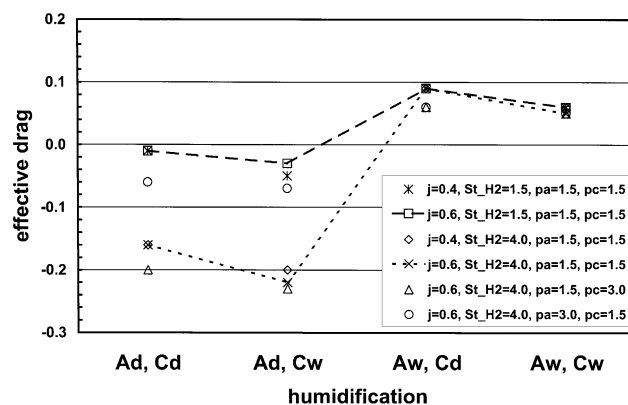
Table 1
The composition of the MEAs investigated in this study

Denomination	Anode	Membrane	Cathode
Base	E-TEK DS	Nafion 105	E-TEK DS
Nafion 112	E-TEK DS	Nafion 112	E-TEK DS
Toray/Toray	Toray + ECN ink	Nafion 105	Toray + ECN ink
E-TEK/Toray	E-TEK DS	Nafion 105	Toray + ECN ink
Toray/E-TEK	Toray + ECN ink	Nafion 105	E-TEK DS
E-TEK SS	E-TEK SS	Nafion 105	E-TEK SS

Fig. 3. The effective drag measured at 60°C with a standard MEA. Results are given for $j = 0.4$ and 0.6 A/cm^2, hydrogen stoichiometry 1.5 and 4 bar, anode pressure 1.5 and 3 bar, cathode pressure 1.5 and 3 bar. The air stoichiometry was 2 in all measurements. The humidification refers to the condition of the anode (A) and cathode (C) inlet gases: 'd' indicates that dry gas was used; 'w' refers to saturated gas. The lines are only drawn to guide the eye: here they are used to emphasise the role of the hydrogen stoichiometry.

The value for the net drag obtained with fully humidified gases (Fig. 3 (A_w, C_w)) was much smaller than the values of 1–2.5 reported for the electro-osmotic drag [11–13] of Nafion membranes with an equivalent weight of 1100. For Nafion membranes with an equivalent weight of 1000, the electro-osmotic drag is certainly not expected to be smaller, since the water content of a Nafion membrane increases with decreasing equivalent weight [14,15] and the electro-osmotic drag increases with the water content [13]. The low values mean that almost all water dragged to the cathode was transported back to the anode. The product water was transported through the cathode to the oxidant flow. The net drag was insufficient to lead to drying out of the anode; the anode gas left the cell fully saturated. Fig. 3 also shows that with these humidification conditions the drag was insensitive to changes in operating conditions such as current density, pressure differences across the MEA, and hydrogen stoichiometry. In the literature [2], it has been suggested that the back transport is determined by Darcy flow, i.e. by a pressure difference between anode and cathode, and therefore is largely independent on the current density. The results here show the opposite tendencies: the differential pressure has no effect and the back transport scales with the current density. The effect of increasing the air stoichiometry was not measured at this temperature.

When the cathode inlet was dry (Fig. 3 (A_w, C_d)), slightly more water was transported from the anode to the cathode. When dry cathode gas entered the cell, it was first of all humidified by product water. In the region of the cathode inlet additional water was drawn from the anode. Note that in the counter-flow configuration used in these experiments, the cathode inlet region is opposite to the anode outlet region (Fig. 1). As a result the relative humidity of the gas at the anode, exit was reduced to 93% when a hydrogen stoichiometry of 4 was used, and even to 61% in the case of $\lambda_{H_2} = 1.5$. Changes in the current density did not affect the measured drag, which means that also with dry inlet air the average water flux through the cathode and anode scaled with the current density. A small reduction of the drag was found when a pressure difference was applied, regardless of the sign of the difference. A higher pressure at the cathode would result in a more rapid saturation, so in this case a decrease was expected. An increase of the anode pressure means that there is less water present at the anode and the drying out of the anode will sooner occur and slow down the transport to the membrane. A low hydrogen stoichiometry should have a similar effect, but this was not observed. However, in both cases the amount of water found at the anode was small and the net drag had large relative error. The effect of the air stoichiometry was not investigated, as at higher stoichiometry, the performance became unstable.

Negative values for the drag were obtained when dry anode gas (Fig. 3 (A_d, C_w)) was fed to the cell. This means product water was drawn to the anode. The most negative values were obtained in the case of large hydrogen stoichiometry and a low anode pressure when the anode could absorb

more water before becoming saturated. The drag was sufficient for a saturated or nearly saturated anode outlet gas. It is well possible that near the anode inlet additional water was drawn from the cathode flow, but due to the large amount of water present at the cathode outlet this does not result in dehydration. As in the previous cases, the influence on the drag of the current density was small, and increase of the cathode pressure led to a small reduction.

When both gases entered the cell dry (Fig. 3 (A_d, C_d)), a small increase in the drag was found compared to the case, where only the hydrogen was dry. Fig. 2 shows that for $\lambda_{H_2} = 1.5$, the amount of product water would be sufficient to saturate both the anode and the cathode. In this experiment, however, the relative humidity at the anode exit was 31% and 143% at the cathode exit. In the case of $\lambda_{H_2} = 4$, the amount of water produced was not sufficient to saturate all gases. Here, however, the relative humidity at the anode and cathode exits was 73 and 105%, respectively. This demonstrates that a large, dry fuel flow can be more effective in absorbing water, that is redundant near the cathode outlet, and therefore can establish a more even distribution of the humidity in the cell. Note that in this respect, there is an optimum for the hydrogen stoichiometry, a too high hydrogen stoichiometry would lead to dehydration of the cathode.

4.2. Base cell performance

Table 2 contains the measured cell voltages at the four inlet humidification conditions. The results for $j = 0.4$ A/cm^2 and $\lambda_{H_2} = 1.5$ show that the cell performance was 40–60 mV lower when saturated cathode gas was replaced by dry cathode gas. A remarkable result was, that with $\lambda_{H_2} = 4$, the performance with dry air/saturated fuel became comparable to the performance with saturated gases. The cause of this improvement is the higher humidity observed at the anode outlet in the case of $\lambda_{H_2} = 4$. As will be shown in [9] by modelling studies, the water activity in the membrane is usually lowest at the anode side, since the electro-osmotic drag and the water production both produce a positive

Table 2
The cell voltage (mV) of the base case MEA[a] at 60°C, measured with different inlet humidification conditions[b,c]

j (A/cm^2)	λ_{H_2}	A_w, C_w	A_w, C_d	A_d, C_w	A_d, C_d
0.4	1.5	630	565	617	568
0.4	4	647	647	642	600
0.6	1.5	545	500	513	488
0.6	4	573	579	577	500

[a] In fact two equivalent MEAs were used: one for the measurements with $\lambda_{H_2} = 1.5$ and one for the measurements with $\lambda_{H_2} = 4$. This explains the difference found between the performances with saturated gases in both channels (A_w, C_w).

[b] A_w: fuel inlet gas humidified; A_d: fuel inlet gas dry; C_w: air inlet saturated; C_d: air inlet dry.

[c] The air stoichiometry was 2 in all cases and the gas pressure 1.5 bar in both channels.

contribution to the gradient of the water activity in the direction from anode to cathode. Hence, a high humidity at the anode can help to prevent drying out of the membrane, in spite of the presence of dry gas at cathode. This mechanism is most efficient when a saturated fuel flow is used. In that case the higher the fuel flow the more water can be transported to the cathode without dehydrating the anode. When dry fuel is used with a low stoichiometry, it will become rapidly saturated but also dehydrate quickly. Dry fuel with a high stoichiometry will not take up sufficient water. This is in agreement with the values of the humidity of the outlet fuel reported in Section 4.1.

Contrary to what was found when dry air was fed to the cell, operation on dry anode gas only led to small decreases of the performance, also at high hydrogen stoichiometry. Since, as explained above, the anode side of the membrane contains less water than the cathode side, it was expected that the membrane would sooner dry out with dry fuel than with dry air. An explanation for the observation that the cell performance suffers more from operation with dry air, may be found in the fact that most activation losses are at the cathode. One of the sources of the activation loss is the slow proton transport through the catalyst layer [16]. Drying out of the catalyst layer will aggravate this loss. In a well-humidified cell activation losses are in the order of 200 mV, e.g. [16]. If we assume that the membrane conductivity in the fully humidified state is in the order of 0.1 s/cm [15] and the membrane thickness is 125 μm, then at 0.4 A/cm^2, the nominal loss due to the membrane resistance is 50 mV. A small fractional increase of the activation energy is therefore more serious than a similar fractional increase of the membrane resistance.

Table 2 also contains results for $j = 0.6$ A/cm^2. Here, similar effects were observed with respect to the humidification and the hydrogen stoichiometry. Note that the voltage loss found when saturated air was replaced by dry air was smaller than for $j = 0.4$ A/cm^2. At a higher current density more water will accumulate at the cathode/membrane interface, leading to a locally higher water content and probably smaller activation losses. The effective drag was not sensitive to the current density (Fig. 3), so the fluxes through membrane and cathode scale equally.

4.3. Nafion 112 membrane

A Nafion 112 membrane is much thinner than a Nafion 105 membrane. The membrane thickness will have a profound effect on the back transport, since with a thinner membrane similar boundary conditions result in larger gradients across the membrane. However, Nafion 1100 has a higher equivalent weight, and as referred to previously, a lower water content. It must be expected that the electro-osmotic drag is slightly smaller in Nafion 112 than in Nafion 105, but this will at least in part be compensated by a smaller value for the permeability, which is likely to decrease with decreasing water content. Therefore, it was expected that in
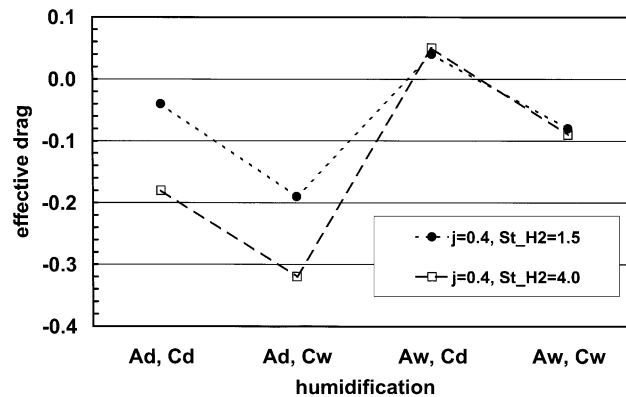

Fig. 4. The effective drag measured at 60°C with a MEA with a Nafion 112 membrane and standard E-TEK electrodes. Results are given for $j = 0.4$, hydrogen stoichiometry 1.5 and 4 bar, gas pressures 1.5 bar. The air stoichiometry was 2 in all measurements. The humidification of the inlet gases was varied (see Fig. 3).

general the net drag would decrease. This is confirmed by the data displayed in Fig. 4. Compared to the corresponding cases measured with a Nafion 105 membrane, the effective drag was about 0.02–0.04 lower in the cases with dry cathode gas, and about 0.15 lower in the cases with wet cathode gas. In the latter cases, the outlet anode gas was extremely wet, i.e. equivalent to a relative humidity >300%. Increase of the hydrogen stoichiometry had a similar effect as for the thicker membrane, i.e. a lower drag when the anode gas was dry.

In Table 3, the performances measured with this cell are listed. Comparison with Table 2 shows that the Nafion 112 cell had a higher performance and was less sensitive to humidification of the inlet gas. For dry cathode/wet anode or dry gases the faster humidification from the anode side resulted in an additional improvement. The favourable effect of a higher hydrogen stoichiometry that was observed for the base cell was not so distinctly present here. On the contrary, a reduction the cell voltage was observed in the case of dry anode/saturated cathode gas. In this case a very negative drag was observed, which may have resulted in a local dehydration of the cathode electrode.

4.4. Alternative electrodes

The use of alternative electrodes (Toray, E-TEK SS) had only a minor effect on the water transport. In general a slight

Table 3
The cell voltage (mV) of the 'Nafion 112-MEA' at 60°C, measured with different inlet humidification conditions[a,b]

j (A/cm^2)	λ_{H_2}	A_w, C_w	A_w, C_d	A_d, C_w	A_d, C_d
0.4	1.5	668	669	672	641
0.4	4	674	674	656	656

[a] A_w: fuel inlet gas humidified; A_d: fuel inlet gas dry; C_w: air inlet saturated; C_d: air inlet dry.
[b] The air stoichiometry was 2 in all cases and the gas pressure 1.5 bar in both channels.
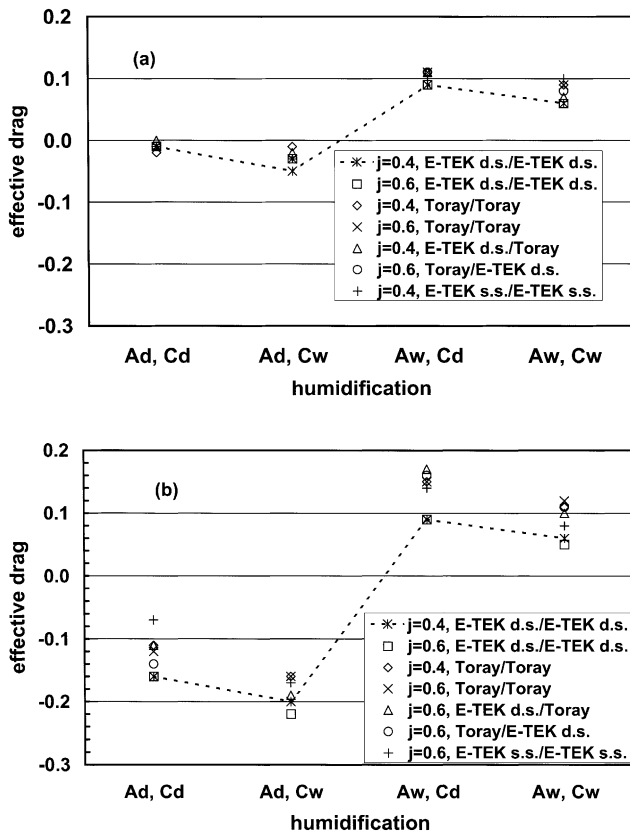
Fig. 5. The effective drag measured at 60°C with several MEAs containing a Nafion 105 membrane but different electrodes. The first electrode in the legend refers to the anode, the second to the cathode. The results obtained with hydrogen stoichiometry 1.5 are shown in (a) and with hydrogen stoichiometry 4 in (b). The air stoichiometry was 2 and gas pressures 1.5 bar. The humidification of the inlet gases was varied (see Fig. 3).

increase of the effective drag was found, i.e. a reduction of the back transport of water (Fig. 5). This increase was more pronounced in the case of a high hydrogen stoichiometry. Large differences in the net drag between the MEAs, e.g. between Toray and E-TEK SS or between the E-TEK DS/Toray combination cells were not observed. The difference between the E-TEK SS and E-TEK DS electrode consists only of an additional microporous hydrophobic layer that is

applied on E-TEK DS at the side of the gas channel. The Toray paper has a different structure, but is also hydrophobic. Staiti et al. [6] investigated the water transport in MEAs containing Toray paper electrodes with varying loads of the hydrophobic agent fluoroethylenepropylene (FEP). They found a clear increase of the net drag with decreasing FEP loading. The drag they obtained with the highest FEP loading (61%) was comparable to the values obtained with standard Prototech electrodes, which are similar to the E-TEK electrodes. This seems in agreement with the present results, which show little difference in the net drag when hydrophobic electrodes are used. No measurements were carried out to investigate explicitly the effect of the thickness of the electrodes. The effective thickness was determined by the thickness of the gaskets, which were chosen in each case to ensure a gas-tight cell. The minimum effective thickness was obtained in the Toray/Toray cell (0.15 mm) and the maximum thickness the E-TEK/E-TEK MEA (0.30 mm), so the possibility that the slight increases obtained for the drag might be caused by a smaller effective thickness of the electrode must be considered.

Although the water transport was similar in all these MEAs, there was a large variation in the measured cell performances, as can be observed from Table 4. The usually observed behaviour in our laboratory is that, when operated with saturated gases, Toray/Toray MEAs perform better than the base case MEA at current densities <0.5 A/cm^2 and worse at higher current densities. The E-TEK SS/E-TEK SS MEAs have a performance similar to the base case MEA at low current density, but are much better at current densities >0.8 A/cm^2, a result also observed in [17]. With E-TEK SS, electrodes current densities up to 1.5–2 A/cm^2 can be obtained which means that E-TEK SS allows effective removal of water from the membrane to the gas channel.

The values in Table 4 are in agreement with these observations. However, when operated with dry air and a H$_2$ stoichiometry of 1.5, the MEAs equipped with E-TEK SS electrodes had a very unstable cell performance and the MEAs with a Toray/ECN cathode showed a voltage loss in the order of 200 mV compared to operation with saturated air. In fact, at larger current densities the cell voltage of this

Table 4
The cell voltage (mV) of the MEA's with alternative electrodes measured with different inlet humidification conditions[a,b]

Anode/cathode	j (A/cm^2)	λ_{H_2}	A$_w$, C$_w$	A$_w$, C$_d$	A$_d$, C$_w$	A$_d$, C$_d$
E-TEK SS/E-TEK SS	0.4	1.5	626	Unstable	621	Unstable
Toray/Toray	0.4	1.5	685	483	685	491
E-TEK DS/Toray	0.4	1.5	679	480	679	457
Toray/E-TEK DS	0.4	1.5	Not measured	599	Not measured	613
E-TEK SS/E-TEK SS	0.6	4	563	Unstable	516	Unstable
Toray/Toray	0.6	4	556	544	580	572
E-TEK DS/Toray	0.6	4	591	549	572	527
Toray/E-TEK DS	0.6	4	585	557	Not measured	533

[a] A$_w$: fuel inlet gas humidified; A$_d$: fuel inlet gas dry; C$_w$: air inlet saturated; C$_d$: air inlet dry.
[b] The air stoichiometry was 2 in all cases and the gas pressure 1.5 bar in both channels.

MEA also became unstable. The MEA with a Toray anode and E-TEK DS cathode performed much better a these conditions, even better than the base case MEA.

The second section of Table 4 shows the results obtained with a higher hydrogen stoichiometry and a higher current density. The cells with a Toray/ECN cathode showed considerable improvement when operation with dry air was performed in combination with a higher hydrogen stoichiometry. This is in agreement with the observation made for the base case MEA above: a high hydrogen stoichiometry provides a large reservoir of water for fast humidification of the cathode inlet gas. A larger hydrogen stoichiometry, however, did not improve the performance of the MEA with E-TEK SS electrodes. With dry cathode gas this MEA was still unstable.

These results suggest that not an increase of the membrane resistance, which should be similar in all cases, but cathode activation losses are mainly responsible for the low cell voltage observed with dry air. In this respect, it seems the catalyst layers in the Toray/ECN and especially the E-TEK SS electrode are much more sensitive to drying-out phenomena at the cathode than the catalyst layer in the E-TEK DS electrode. As the catalyst layers in E-TEK SS and E-TEK DS electrodes have similar composition and structure, it must be concluded that the presence of an additional hydrophobic microporous layer in E-TEK DS is beneficial for the humidification of the cathode catalyst layer, i.e. it presents a buffer between the dry gas channel and the wet membrane. In a recent study by Jordan et al. [18], the role of a gas diffusion layer next to the catalyst layer in avoiding flooding or drying out of the catalyst was demonstrated. The present work shows the importance of such a layer facing the gas channel when dry air is being used. In the case of wet cathode gas, this layer probably obstructs the removal of liquid water leading to large diffusion losses at the cathode and a reduced performance when $j > 1$ A/cm^2. With an E-TEK SS cathode, on the other hand, current densities in the order of 1.5–2 A/cm^2 can be obtained at saturated conditions.

The structure of the Toray paper is quite different. It was already known that with Toray only limited current densities can be obtained at saturated conditions, since condensation in the pores causes diffusion losses, and now it is found that operation with dry air also can lead to severe losses. The above results show that by careful selection of, e.g. the anode conditions the losses may be reduced but it seems that for cells equipped with Toray electrodes operating conditions should always be carefully chosen.

4.5. Measurements at 80°C

A base case MEA was also studied at 80°C. The net drag obtained with saturated gases was larger than at 60°C (Fig. 6), but smaller than the r_{max}, which according to Eq. (11) is 0.24 at 1.5 bar, so the anode remained saturated. Also, at this temperature no significant effect of the current density was observed. The stoichiometry of the saturated
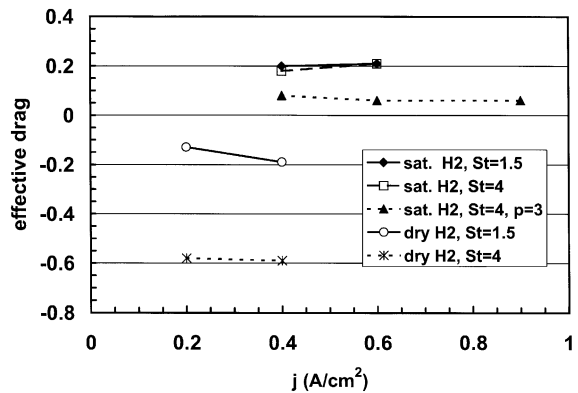

Fig. 6. The effective drag measured at 80°C with a standard MEA as function of the current density. Results are given for gas pressures 1.5 bar in both channels except for one set of measurements carried out with $p = 3$ bar in both channels. The hydrogen stoichiometry and the hydrogen humidification were varied.

gases does not affect the net drag, as is shown for the hydrogen stoichiometry. Additional measurements with a larger air stoichiometry, to 5, also gave unchanged results.

Operation with dry anode gas resulted in limited losses, in agreement with the results obtained at 60°C. The drag obtained with dry anode gas was much more negative than at 60°C. Increase of the stoichiometry of the anode gas led to a further reduction of the drag to less than −0.5, meaning that in addition to all the product water, some water from cathode gas was drawn to the anode. Again, it was found that the back transport through the membrane is mainly determined by the conditions in the anode gas channel, and that the back transport can easily cancel the electro-osmotic drag.

It was not possible to operate the base case MEA at this temperature and at 1.5 bar with dry air, not even in combination with a saturated inlet hydrogen flow with $\lambda_{H_2} = 4$. The reason for this is of course that at 60°C most of the water needed to saturate the air can be supplied by the product water. At 80°C, a larger contribution from the anode is required and this results in drying out of the anode gas.

In Fig. 6 there are also points included measured with a gas pressure of 3 bar, both at the anode and at the cathode. This led to a reduction of the effective drag, again till just below the value of r_{max} (Eq. (11)). In fact, all measurements with the base case MEA at 80°C as well as at 60°C show that the back transport of water is always such that it results in a saturated anode. If for simplicity the electro-osmotic drag is assumed to be independent of pressure and temperature, this means that back transport becomes smaller as the temperature increases and increases at increased pressure. This indicates that the gas conditions play a crucial role in the water transport.

5. Conclusions

The water transport in a PEMFC, characterised by the net or effective drag in a cell, has been experimentally

investigated for a range of conditions and materials. A large data set was obtained, which was used to identify the main factors that govern the water transport. Secondly, a correlation between the water transport and the cell performance could be made.

Analysis of these data has shown that the effective drag is determined by the following three factors.

1. The humidity of the inlet gases.
2. The conditions that determine the humidity along the gas channel, i.e. stoichiometry, temperature and pressure.
3. The thickness of the membrane.

The tendency of gases to take up water to saturation level explains many of the observations made. The outlet anode gas was always saturated, except where the anode outlet was opposite a dry cathode inlet, where water was drawn from the anode to the cathode. The effective drag did not depend significantly on the current density (at fixed stoichiometry). The effect of a differential pressure across the membrane could be explained in terms of changes in the gas humidity rather than in terms of Darcy flow. Finally, the net drag did not depend significantly on the electrode materials. This was ascribed to the highly hydrophobic character of the electrodes.

The cell performance was also very sensitive to the humidity of the inlet gases. Drying-out phenomena at the cathode side were much more detrimental for the cell performance than at the anode side, which indicates that the increase of activation losses was much larger than the increase of the membrane resistance. The severity of the drying-out depended very much on the cathode electrode material: with E-TEK SS operation with dry air was not possible. When Toray paper was used at the cathode, operation with dry air was only possible at a limited set of conditions. In several cases, it was found that drying out of the cathode could be avoided by increasing the amount of water in the anode gas, a fact that may be of practical use when reformate gas is being used as fuel.

The results presented here show that the water management in PEMFCs requires careful consideration, especially when they are operated in a stack where the conditions may not always be well controlled. Moreover, the response to a change in the conditions that govern the water transport depends strongly on composition of the MEA. Additional research is necessary to establish the importance of the activation losses versus the membrane losses and the role played by the electrode material and structure, in order to

get a clear picture of all the drying-out phenomena that occur in a PEMFC.

The effective or net drag of course gives only limited information on the distribution of the humidity in the cell and therefore the conclusions with respect to the origin of the cell performance loss contain a fair amount of conjecture. In another paper [9], a two-dimensional model will be presented that allows the translation of the effective drag data to information on local water fluxes, enabling a more accurate description of the observed cell behaviour. Such a model will be of use to further clarify the water management problems that occur in a PEMFC and to make predictions for different materials and conditions.

References

[1] D.M. Bernardi, M.W. Verbrugge, J. Electrochem. Soc. 139 (1992) 2477–2490.
[2] M. Eikerling, A.A. Kornyshev, Y. Kharkats, Y. Volfkovich, J. Electrochem. Soc. 145 (1998) 2684–2698.
[3] T.F. Fuller, J. Newman, J. Electrochem. Soc. 140 (1993) 1218–1225.
[4] T. Okada, G. Xie, M. Meeg, Electrochim. Acta 43 (1998) 2141–2155.
[5] T.E. Springer, T.A. Zawodzinski, S. Gottesfeld, J. Electrochem. Soc. 138 (1991) 2334–2342.
[6] P. Staiti, Z. Poltarzewski, V. Alderucci, G. Maggio, N. Giordano, A. Fasulo, J. Appl. Electrochem. 22 (1992) 663–667.
[7] F.N. Buechi, S. Srinivasan, J. Electrochem. Soc. 144 (1997) 2767–2772.
[8] K.-H. Choi, D.-H. Peck, C.S. Kim, D.-R. Shin, T.-H. Lee, J. Power Sources 86 (2000) 197–201.
[9] G.J.M. Janssen, J. Electrochem. Soc., submitted for publication.
[10] T.A. Zawodzinski, T.E. Springer, F. Uribe, S. Gottesfeld, Solid State Ionics 60 (1993) 199–211.
[11] T.F. Fuller, J. Newman, J. Electrochem. Soc. 139 (1992) 1332–1336.
[12] T.A. Zawodzinski, J. Davey, J.A. Valerio, S. Gottesfeld, Electrochim. Acta 40 (1995) 297–302.
[13] M. Ise, K.D. Kreuer, J. Maier, Solid State Ionics 125 (1999) 213–223.
[14] F.N. Buechi, M. Wakizoe, S. Srinivasan, J. Electrochem. Soc. 143 (1996) 927–932.
[15] J. Huslage, F.N. Buechi, G.G. Scherer, in: C. Daum, J. Leuenberger (Eds.), Paul Scherrer Institute Scientific Report 1998, Vol. V, General Energy, Paul Scherrer Institute (PSI), Villigen, Switzerland, 1999, pp. 55–56.
[16] T.E. Springer, T.A. Zawodzinski, M.S. Wilson, S. Gottesfeld, J. Electrochem. Soc. 143 (1996) 587–599.
[17] B. Mueller, T. Zawodzinski, J. Bauman, F. Uribe, S. Gottesfeld, M. De Marinis, E. De Castro, in: S. Gottesfeld, T.F. Fuller, G. Halpert (Eds.), Proton Conducting Membrane Fuel Cells, Proceedings of the 2nd International Symposium, PV 98-27, The Electrochemical Society Proceedings Series, Pennington, NJ, 1999, pp. 1–9.
[18] L.R. Jordan, A.K. Shukla, T. Behrsing, N.R. Avery, B.C. Muddle, M. Forsyth, J. Power Sources 86 (2000) 250–254.